Journal of Hazardous Materials 184 (2010) 425–431

Contents lists available at ScienceDirect

Journal of Hazardous Materials

journal homepage: www.elsevier.com/locate/jhazmat

Chromium VI adsorption on cerium oxide nanoparticles and morphology changes during the process

Sonia Recillas[a], Joan Colón[a], Eudald Casals[b], Edgar González[b], Victor Puntes[b,c], Antoni Sánchez[a,*], Xavier Font[a]

[a] Department of Chemical Engineering, Engineering School, Autonomous University of Barcelona, 08193 Bellaterra, Spain
[b] Catalan Institute of Nanotechnology, Autonomous University of Barcelona Campus, 08193 Bellaterra, Spain
[c] Catalan Institute of Research and Advanced Studies, Passeig Lluís Companys, 23, 08010 Barcelona, Spain

ARTICLE INFO

Article history:
Received 18 May 2010
Received in revised form 27 July 2010
Accepted 15 August 2010
Available online 21 August 2010

Keywords:
CeO_2 nanoparticles
Adsorption
Desorption
Kinetics
Chromium VI
Toxicity

ABSTRACT

In this study, suspended cerium oxide nanoparticles stabilized with hexamethylenetetramine were used for the removal of dissolved chromium VI in pure water. Several concentrations of adsorbent and adsorbate were tested, trying to cover a large range of possible real conditions. Results showed that the Freundlich isotherm represented well the adsorption equilibrium reached between nanoparticles and chromium, whereas adsorption kinetics could be modeled by a pseudo-second-order expression. The separation of chromium–cerium nanoparticles from the medium and the desorption of chromium using sodium hydroxide without cerium losses was obtained. Nanoparticles agglomeration and morphological changes during the adsorption–desorption process were observed by TEM. Another remarkable result obtained in this study is the low toxicity in the water treated by nanoparticles measured by the Microtox® commercial method. These results can be used to propose this treatment sequence for a clean and simple removal of drinking water or wastewater re-use when a high toxicity heavy metal such as chromium VI is the responsible for water pollution.

1. Introduction

Water treatment is one of the main health concerns around the world. The world's supply of fresh water is running out. Already one person in five has no access to safe drinking-water. Improving access to safe drinking-water can result in tangible improvements to health. Therefore the development of new technologies to improve process of products in the area of water treatment is fundamental. One of the promising technologies is based on nanotechnology devices and products. Nanotechnology is the engineering of functional systems at the molecular scale, synthesized "bottom-up", which offer new products and process alternatives for water purification, being the advantage of these materials the large surface to volume ratio [1].

Some examples of nanodevices proved in water treatment are based on nanoparticles, nanomembranes, bioactive nanoparticles, carbon nanotubes and nanofibers [2–5]. In the future, the impact of these nanomaterials on human health and environment would be critical issues involving the materials and process selection for water purification on large scale [6].

Chromium (VI) is one of the contaminants that has been used as target pollutant due to its high toxicity and also for the well-documented human health problems associated to chromium [7]. The amount of chromium (Cr) allowed in purified water is very low (50 μg/l according to the Council of the European Union [8]). A variety of products and processes have been used for chromium removal in water [9]; nevertheless the adsorption process is one of the more effective and versatile techniques for Cr removal from water and when combined with an appropriate desorption step the problem of sludge disposal could be solved [10]. The absorbents used for Cr(VI) removal are alumina, silica [11,12], activated carbon [13,14] or natural adsorbents [15]. In the field of nanotechnology amino-functionalized magnetic nanoadsorbents [16], iron nanoparticles, cerium micro/nanocomposite structures [17] or carbon nanotubes supporting cerium nanoparticles [18] have been used. Cerium nanocrystal microspheres [19] have been also synthesized and tested with the same objective.

Cerium nanoparticles have been used in a variety of industrial applications such as catalysis, solar energy devices, optical display technology and corrosion prevention [20,21]. All of these applications are related with chemical reaction at the surface, while cerium nanoparticles reactivity is correlated to surface defects.

* Corresponding author. Tel.: +34 93 5811019; fax: +34 93 5812013.
E-mail addresses: antoni.sanchez@uab.cat, antoni.sanchez@uab.es (A. Sánchez).

0304-3894/$ – see front matter © 2010 Elsevier B.V. All rights reserved.
doi:10.1016/j.jhazmat.2010.08.052

Another important issue is to determine the toxicity of the synthesized materials and the prevention of future environmental damages. The Microtox® assay based on the use of bioluminescent marine bacterium, *Photobacterium phosphoreum/Vibrio fischeri*, adopted for the assessment of toxicity of polluted water [22] is commonly used to test detoxification efficiency.

In the present paper CeO_2 nanoparticles (6.5 nm mean size) were synthesized and fully characterized to be used as adsorbent for the removal of chromium (VI) from pure water solutions. The adsorption isotherms at 0.6, 37.5, 80 mg/l initial chromium (VI) concentrations were obtained and different eluents were tested for the chromium (VI) desorption. Because the application would be for dinking or natural water treatment technologies, the experiments were performed at pH = 7. The changes in morphology during the adsorption–desorption process were studied by transmission electron microscopy. The toxicity of the decontaminated effluents was also studied using the Microtox assay to evaluate the overall possibilities of this treatment.

2. Materials and methods

2.1. CeO_2 nanoparticles preparation

CeO_2 nanoparticles were synthesized in aqueous phase, using milli-Q grade water. All reagents were purchased from Sigma-Aldrich and used as received. All the synthesis procedures are based in preexisted ones available in the scientific literature with modifications to be adapted to large-scale yields. Briefly, CeO_2 nanoparticles synthesis was based on Zhang et al. [23]. The Ce^{3+} ions from $Ce(NO_3)_3$ salt are oxidized at basic pH conditions to Ce^{4+} using hexamethylenetetramine (HMT). Specifically, stock solutions of 1 M of both reactants were prepared and stored at room temperature. Afterwards, both were mixed and stirred during 24 h at final concentrations of 37.5 mM for $Ce(NO_3)_3{\cdot}6H_2O$ and 0.5 M for HMT, under mild stirring and room temperature conditions. In this process, CeO_2 nanocrystals form and the same reagent (HMT) stabilize them in aqueous medium, forming the double electrical layer to prevent nanoparticles agglomeration.

2.2. Characterization and stability of nanoparticles

For the fully characterization of nanoparticles, the obtained nanoparticles suspension was analyzed with dynamic light scattering (DLS) to determine the nanoparticles size distribution (and therefore if agglomeration had occurred) in a Nanoparticle Analysis System (Malvern, UK). DLS is a well-known tool to determine the hydrodynamic diameter of colloidal particles.

Zeta potential (ZP) measurements were also performed to study some surface properties and changes after the experiments. ZP is a useful technique to study nanoparticles stability and their surface charge in colloids when they are electrostatically stabilized.

X-ray diffraction spectra (using a PANalytical X'Pert diffractometer with a Cu Kα radiation source) have also been taken to determine the crystalline phase of the samples.

The dissolved cerium concentration from the desorption experiments was obtained by inductively coupled plasma mass spectrometry (ICP-MS) using an Agilent Equipment (Model 7500ce).

Transmission electron microscope (TEM, using a JEOL 1010 operating at an accelerating voltage of 80 kV) images of the samples were also taken after nanoparticles synthesis, to characterize the nanoparticles before and after the chromium adsorption process.

Table 1 shows some of the main characteristics of the used nanoparticles as they were synthesized.

Table 1
Main characteristics of the used CeO_2 nanoparticles.

CeO_2 nanoparticle	
Concentration (mg/ml)	0.64
Mean size (nm)	12
Shape	Shapeless
Zeta potential (mV)	+11.5
Stabilizer[a]	HMT
Stabilizer concentration (mM)	8.3
pH (original)	9
Surface BET area (m^2/g)	65

[a] HMT, hexamethyltetramine.

2.3. Cr(VI) adsorption studies

The adsorption kinetics, the maximum adsorption capacity (q_e) of CeO_2 nanoparticles synthesized at different initial concentrations of chromium (VI) at pH = 7, were performed using the following procedure: chromium (VI) solutions were prepared dissolving $K_2Cr_2O_7$ in deionized water and performing the corresponding dilutions to obtain 0.6, 37.5 and 80 mg/l solutions. The pH of each solution was adjusted at 7 using sodium hydroxide 1 M. Each of these solutions was added to equal volumes of CeO_2 nanoparticles suspension adjusted to pH = 7 and then the solutions were continuously stirred at 150 rpm at room temperature. Final concentration of CeO_2 nanoparticles was 320 mg/l. Samples were taken at different times, separated by centrifugation and Cr(VI) was analyzed in the liquid phase.

The method used for the determination of chromium total was the standard colorimetric method used for the examination of water and wastewater [24]. The chromium VI concentration is determined colorimetrically by reaction with diphenylcarbacide in acid solution. The reaction is very sensitive; being the molar absorptivity based on chromium about 40,000 $l\,g^{-1}\,cm^{-1}$ at 540 nm. To determine total chromium, the sample was digested with a sulphuric–nitric acid mixture to oxidize with potassium permanganate before reacting with the diphenylcarbazide. The determination of trivalent chromium on the liquid phase was performed by oxidation with potassium permanganate as follow: 1 ml of sample was added into a 125 ml conical flask. Acid sulphuric–nitric (1:1, v:v) solution was added dropwise until the solution is acid, plus 1 ml in excess, the volume was adjusted to 40 ml and heat to boiling. Two drops of $KMnO_4$ solution were added and the resulting solution was boiled for 2 min more. 1 ml NaN_3 solution was added. The sample continued boiling for 1 min after colour has faded completely. The sample was cooled and then the process for the determination of Cr VI is performed. The chromium IV determination was obtained as follow: 1 ml of sample was added into a 100 ml flask, 0.25 ml H_3PO_4 was added and the pH was adjusted to 1.0 ± 0.3 with a 0.2 N H_2SO_4 solution. The solution was transferred to a 100 ml flask, diluted to 100 ml, and mixed. 2.0 ml diphenylcarbazide solution was added, mixed and wait for 10 min for full colour development. An appropriate portion of the sample was transfer to a 1-cm absorption cell and its absorbance was measured at 540 nm. The amount of Cr III in solution will be the difference between total chromium (with oxidation step) and the Cr VI amount. No difference between the Cr VI and Cr total was obtained in the liquid phase after centrifugation.

Experiments were carried out in triplicate and the average values are presented. Standard deviation was very low (less than 5% in all cases) and it is not presented.

2.4. Cr(VI) desorption studies

Desorption study was performed using the following procedure. Samples of 0.7 ml of a suspension of 640 mg/l CeO_2 nanoparti-

cles previously adjusted at pH = 7 were shaken and then 0.7 ml of 80 mg/l of chromium (VI) solution were added. The suspensions were stirred for 3 h at 150 rpm at room temperature and then separated by centrifugation. In three samples chromium (VI) was determined at the liquid phase. In the remaining 15 samples, the solid phases were dried at room temperature for 24 h. 1 ml of each eluent used (deionized H_2O, 0.1 M HNO_3, 0.1 M HCl, 0.1 M H_2SO_4 and 0.1 M NaOH) were added to the solid samples and then the suspensions were stirred for 3 h, separated by centrifugation and chromium (VI) was analyzed in the liquid phase. The initial and final concentrations of chromium (VI) were obtained by the same analytical method used for adsorptions studies. The amount of cerium in solution was determined by ICP-MS. Experiments were carried out in triplicate and the average values are presented.

2.5. Bioluminescent test

A Microtox Analyzer model 500 from Microbics Corporation was used. Whole Effluent Toxicity (WET) test protocol was used to obtain the toxicity of the initial chromium (VI) solution (30 mg/l), the initial nanoparticles suspension of CeO_2 (320 mg/l) and the final suspension obtained after 3 h of reactions at pH 7 and at room temperature. The Microtox test is based on the percentage of decrease in the amount of light emitted by the bioluminescent marine bacterium *V. fischeri* (*P. phosphoreum*) [22]. The light emitted reduction is directly related to the relative toxicity of the sample. For the three suspensions the half maximal inhibitory concentration (IC_{50}) was calculated. IC_{50} is a measure of the effectiveness of a compound in inhibiting biological or biochemical function and it was obtained from plotting the percentage of luminescence reduction against concentration after 5 and 15 min incubation time. The experimental procedure has been adopted from the official standards of several countries [25,26]. Toxicity tests for stabilizer samples and nanoparticles suspensions samples were performed in triplicate. pH of stabilizers and nanoparticles suspension samples was previously adjusted to 7. No visible precipitate was observed during the adjustment. The procedure used is as follows: The pH of the samples was adjusted at pH 7 with citric acid. 10 ml of samples was added to a vessel containing 0.2 g of NaCl and mixed. 2000 μl of the suspension was added to a tube test. 1000 μl of diluent was added to each test tube. Afterwards, 1000 μl of osmotically adjusted sample was added to test tubes making 1:2 serial dilutions by transferring 1000 μl, mixing after each transfer. After 5 min, a vial of Microtox Acute Toxicity Reagent was reconstituted in the following way: pouring the reconstitution solution (precooled at 4 °C) into the opened vial, swirling the vial 3 or 4 times, then quickly pouring the mixture back into the cuvette. Bacteria were thoroughly mixed using a pipette by aspirating and dispensing 0.5 ml of solution at least 10 times. Reconstituted bacteria should be used within 3 h of reconstitution. Finally, 10 μl reagent are transferred to each test tube and mixed in cuvettes by shaking. I_{15} light levels at 5 min and 15 min can be already read. The sample concentrations performed were 320, 160, 80, 40, 20 mg/ml.

3. Results and discussion

3.1. Adsorption isotherms

CeO_2 nanoparticles crystallize in a cubic fluorite structure and the predominant crystallographic planes exposed at the surface in the synthetic procedure used are the (1 1 1) (Fig. 1), which are responsible of the catalytic behaviour [27]. The average diameter obtained was 11.7 ± 1.6 nm of 6.5 nm (Table 1). The size distribution was obtained after image analysis of different TEM images, counting at least 500 NPs (Fig. 1). These nanocrystals have more

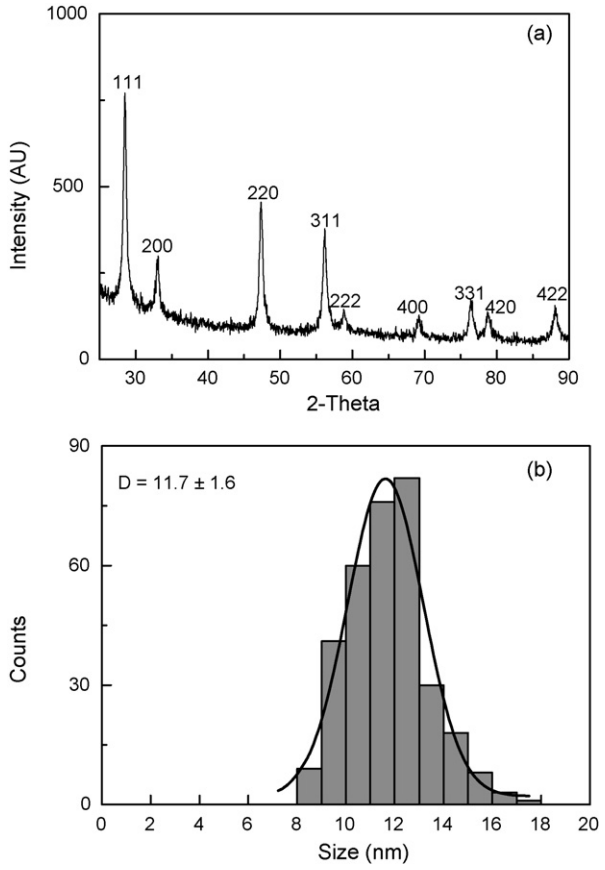

Fig. 1. X-ray diffraction spectra (a) and size distribution (b) of CeO_2 nanoparticles.

cerium atoms per unit of surface than oxygen atoms, inversely to CeO_2 NPs (1 0 0)-terminated which are predominantly oxygen terminated [28]. These are related with the storage and releasing of oxygen, and the promotion of noble-metal activity and dispersion [29,30]. Both phenomena are controlled by the type, size, and distribution of oxygen vacancies as the most relevant surface defects [31,32].

The adsorption evolution through time, obtained at different concentrations of chromium (VI), is shown in Fig. 2. A brown precipitate was observed in each case before the first measure of Cr(VI) was made. In the three chromium concentration cases the equilibrium concentration was reached almost immediately. After 30 min the systems reached equilibrium and were stable with time. The removal efficiency after 4 h of adsorption were found to be 96.5%, 67.8% and 50.6% and the maximum adsorption capacity of

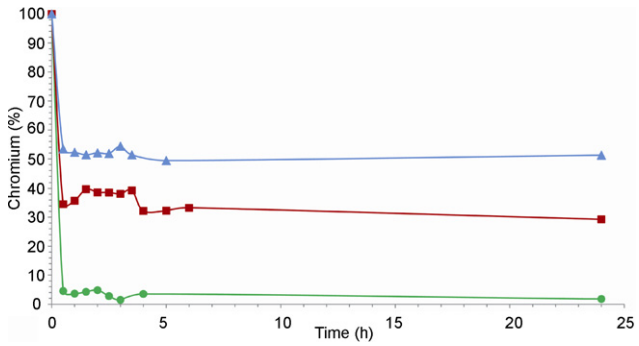

Fig. 2. Chromium adsorption evolution at pH = 7 and room temperature. Initial Cr(VI) concentrations are 0.6 (circle), 37.5 (square), 80 mg/l (triangle).

Cr(VI) obtained after 24 h were 1.88 mg Cr(VI)/g CeO_2 nanoparticles, 83.33 mg Cr(VI)/g CeO_2 nanoparticles and 121.95 mg Cr(VI)/g CeO_2 nanoparticles at the initial concentration of Cr(VI) of 0.6, 37.5, 80 mg/l respectively (Fig. 2). Three samples of CeO_2 NPs with adsorbed chromium were centrifuged and the total amount of chromium and chromium VI were obtained from the liquid and the solid (previous dissolution in acid medium) phases. Cr VI was not detected in the solid phase. The total Cr obtained was chromium III. In the liquor phase only chromium VI was obtained. These results suggest an oxido-reduction process on the surface of the nanoparticle. At these reaction conditions, the reduced chromium is not liberated to the medium; remains on the NPs surface. The presence of Ce^{3+} at the oxygen vacancy has been reported [33].

To compare the adsorption capacity of the CeO_2 nanoparticles synthesized with others adsorbents reported in the literature, the reaction conditions must be similar. In Table 2 some previous values reported in the literature are compared. However, it should be noted that it is not easy comparing adsorption results because the experimental conditions are not the same. The NPs synthesized are not supported under other material, all the surface area are available to adsorption process. Differences in the synthesis process of NPs could change the physico-chemical properties of the surface.

CeO_2 nanoparticles synthesized adsorb 1.88 mg/g at low initial Cr(VI) concentration adsorbate (0.6 g/ml and 320 mg/l Cr(VI) and CeO_2 respectively). This value is higher than the adsorption capacity reported in the literature by Xiao et al. [19] (1.5 mg/l) even though the initial concentration and adsorbate mass were almost two times smaller. At the same equilibrium Cr(VI) concentration (15 mg/l Cr(VI)), Di et al. [18] showed that the adsorption capacity of CeO_2 nanoparticles synthesized were higher than the values reported. Yuan et al. [34] reported the use of montmorillonite-supported magnetite nanoparticles for chromium removal even though the removal efficiency at pH closer to 7 is low. These results suggest the possibility of CeO_2 nanoparticles to be used for water treatment process at pH 7 in a wide range of chromium concentration for drinking water purification (small concentration levels of chromium (VI)) to industrial wastewater treatment process to remove high concentration of chromium. Finally, it must be pointed that HMT, as stabilizer, is added in excess in the reaction bath, while the precursor of cerium atoms, cerium nitrate, is the limiting factor. However, according to literature, HMT easily decomposes to formaldehyde and finally to ammonia ($NH_4^+OH^-$), CO_2 and H_2O [35,36].

The experimental data fit well the Freundlich adsorption isotherm model [29], which represents the relationship between the amount of adsorbate 15.77 adsorbed per unit mass of adsorbent (q_e) and the concentration of adsorbate at equilibrium (C_e), being K and n are constants representing the adsorption capacity and intensity of the adsorption (Eq. (1)):

$$q_e = kC_e^{1/n} \quad (1)$$

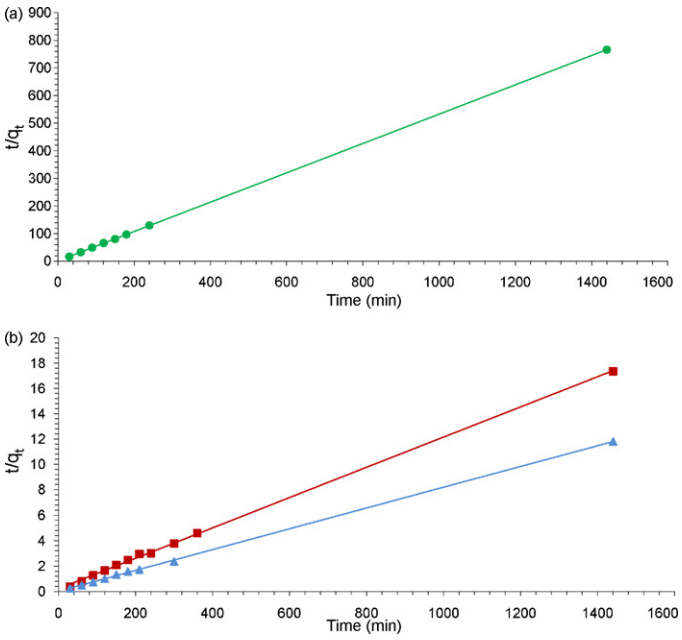

Fig. 3. Adsorption pseudo-second-order kinetic model for chromium adsorption at pH = 7 and room temperature. Initial Cr(VI) concentrations are 0.6 (circle), 37.5 (square), 80 mg/l (triangle).

The correlation coefficient obtained was $R^2 = 0.9554$ and n value was 2.1 and k value was 20.57.

3.2. Pseudo-second-order kinetic model

A pseudo-second-order model based on the assumption that the rate limiting step are the chemical sorption involving valence forces through sharing or the exchange of electrons between sorbent and sorbate [37] was used as kinetic model. The kinetics of the sorption reaction has been described as a function of the sorption equilibrium capacity (q_e), the initial metal ion concentration, the adsorbent dose and the nature of solute ion.

The pseudo-second-order rate constants (k_2) and the amount of Cr(VI) adsorbed at equilibrium (q_e) were calculated experimentally by plotting (t/q_t) versus t according to Eq. (2). q_e is the amount of Cr(VI) adsorbed (mg/g) at equilibrium, and q_t is the amount of the adsorption (mg/g) at any time t. The kinetics of the removal process is shown in Fig. 3.

$$\frac{t}{q_t} = \frac{1}{k_2 q_e^2} + \left(\frac{1}{q_e}\right) t \quad (2)$$

The obtained values fitted well according to this model (Table 3).

Table 2
Maximum chromium (VI) sorption capacity of various adsorbents.

Adsorbent	Adsorbent capacity (mg Cr(VI)/g adsorbent)	Initial Cr(VI) concentration (mg/l)	Equilibrium Cr(VI) concentration (mg/l)	Initial adsorbent concentration (g/l)	References
Synthesized CeO_2 nanoparticles	1.88	0.6		0.320	This work
Synthesized CeO_2 nanoparticles	83.33	37.5		0.320	This work
Synthesized CeO_2 nanoparticles	121.95	80		0.320	This work
Cerium microsphere	1.5	2		1	[18]
Commercial Cerium	0.37				[18]
Synthesized CeO_2 nanoparticles	70.41		15		[17]
CeO_2/ACNTs	26		15		[17]
Activated carbon EA-200	10		15		[17]
γAl_2O_3	7.5		15		[17]

Table 3
Maximum adsorption capacity at equilibrium and pseudo-second-order rate constants (k_2) obtained using the pseudo-second-order kinetic model for 0.6, 37.5 and 80 mg/l initial Cr(VI) concentration.

Cr(VI) initial (mg/l)	q_e (mgCr(VI)/gCeO_2)	k_2 (g CeO_2/ mgCr(VI) min)	R^2
0.6	1.88	0.2525	1
37.5	83.33	0.012	0.9998
80	121.95	0.0082	0.9992

3.3. Cr(VI) desorption studies

The chromium desorption study was performed at neutral, acid and basic conditions (deionized H_2O, 0.1 M HNO_3, 0.1 M HCl, 0.1 M H_2SO_4 and 0.1 M NaOH). The chromium desorption at acid eluents have higher recovery percentage, around 100% with H_2SO_4, 80% recovery with HCl and 86% with HNO_3 (Fig. 4); however a considerable redissolution of CeO_2 was detected (Fig. 4).

The amount of Cr(VI) obtained using water as eluent could be the chromium physically sorbed at the surface when the cerium–chromium particles were dried, before the addition of the eluents. Regarding the cerium detected in deionized water eluent (5% of the initial cerium) it could be due to nanoparticles suspended at the liquid phase. It is evident that Cr VI ionic forms change with pH. However, one of the main advantages of CeO_2 nanoparticles for adsorption process is the wide maximum adsorption as a function of pH (from 3.0 to 7.4) [18]. A slight diminution of pH during the adsorption process was observed, the final pH value after 24 h was 6.5.

The chromium desorption process performed with NaOH as eluent was less efficient (64% recovery) than the acid eluents but the amount of Ce in dissolution was minimum 0.07%. Probably at higher NaOH concentrations higher chromium desorption should be produced; then the CeO_2 nanoparticles could be re-used without a complicated separation process. In fact, After 24 h desorption process treatment with 0.1 M NaOH solution, the NPs were separated by centrifugation process and were re-used for chromium removal (triplicate). 75% of chromium removal was obtained in this second cycle.

According to the obtained results desorption and regeneration of CeO_2 nanoparticles should only be feasible, from a practical point of view, in the case of basic desorption.

3.4. Transmission electron microscopy

Transmission electron microscopy (TEM) images of initial CeO_2 nanoparticles are shown in Fig. 5a and b. Octahedral CeO_2 nanocrystals with a uniform size distribution of 12 nm (Table 1) were obtained. A control sample was also performed without the addition of Cr(VI) solution, with deionization water being used instead, maintaining the same conditions of agitation and time than in the adsorption experiments. These CeO_2 nanoparticles (Fig. 5c) show a fine homogeneous agglomerate of particles around 12 nm of diameter conformed by smaller rounded nanoparticles with homogeneous size and morphology. A change in morphology was observed without the addition of chromium VI solution. The octahedral nanocrystals of the nanoparticles synthesized were not observed in the images of CeO_2 nanoparticles with deionized water added. A diminution of nanoparticles size was also observed. These morphology variations in the nanostructures are attributed to an intra-agglomerate re-orientation to attain the low energy configuration [38]. TEM images of CeO_2 nanoparticles after chromium (VI) adsorption showed the presence of spherical homogeneous interconnected agglomerates with approximately 70 nm in diameter (Fig. 5d). These agglomerates are ensembles of spherical nanoparticles. An estimation of the particle size is possible from a few isolated nanoparticles in the periphery of the agglomerates (Fig. 5e); the diameter particle is in the order of 2 nm. However, an accurate measure of the particle size distribution of these nanoparticles could not be obtained.

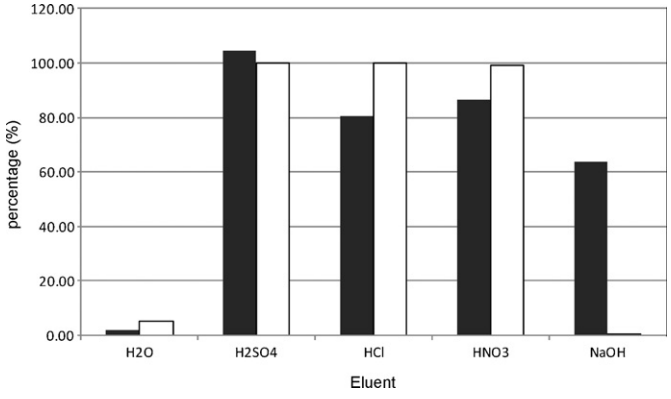

Fig. 4. Chromium (VI) desorption from nanoparticles of CeO_2 after 3 h of reaction with different eluents (black bars) and percentage of the initial cerium dissolved after desorption experiments, analyzed by ICP-MAS (white bars).

Fig. 5f shows the homogeneous agglomeration of CeO_2 nanoparticles obtained after desorption treatment using 0.1 M NaOH as eluent. 80 nm agglomerated diameter and 4 nm nanoparticles approximately in diameter were measured. Electrostatic forces between these particles could result in particle agglomeration.

3.5. Adsorption mechanism

The CeO_2 nanoparticles with a positive charge (Z potential 11.5 mV) were stabilized via electrostatic repulsion with a covered hexamethylenetetramine molecules shell on the particle surface. When the chromium (VI) solution was added to the nanoparticles, a brownish agglomerate was immediately observed. Attractive forces (e.g. induced dipole interaction, Van der Waals force, hydrogen bonds, bi- or multivalent, oppositely charged ions or polyelectrolytes) can bridge the particles by electrostatic attraction, causing destabilization of the nanoparticles [39,40]. In this case the presence of chromium ions in solution could destabilize the nanoparticles dispersion, reacting and forming aggregates. The charge and the species in solution is one of the most important issues in agglomeration phenomena, in the case of chromium (VI) solutions, the solution species are a function of the pH and total Cr concentration [41]. At pH 7 the major species in solution are $HCrO_4^-$ and CrO_4^{2-}. The charge attraction of the chromium anions to the positive charged nanoparticles could be the first step process, then a chemisorption process could proceed and a multibranche homogeneous in size and shape network is formed with the chromium ions acting as a bridge between different CeO_2 nanoparticles surface via an anionic interchange between the ionic chromium species and the hydroxylation surface [10]. Nevertheless, the heterogeneous metal oxide surface, for example oxygen vacancy, step edges [42,43] and small amounts of Ce^{3+} on the surface remaining from the reaction synthesis could contribute to the chromium elimination by chromium reduction process.

The stability of the aggregates formed still remains after basic desorption treatment. In any case, the agglomeration of the CeO_2 nanoparticles provides an easy way to remove the product in order to separate and re-use the CeO_2 nanoparticles and to obtain a concentrated chromium solution by desorption.

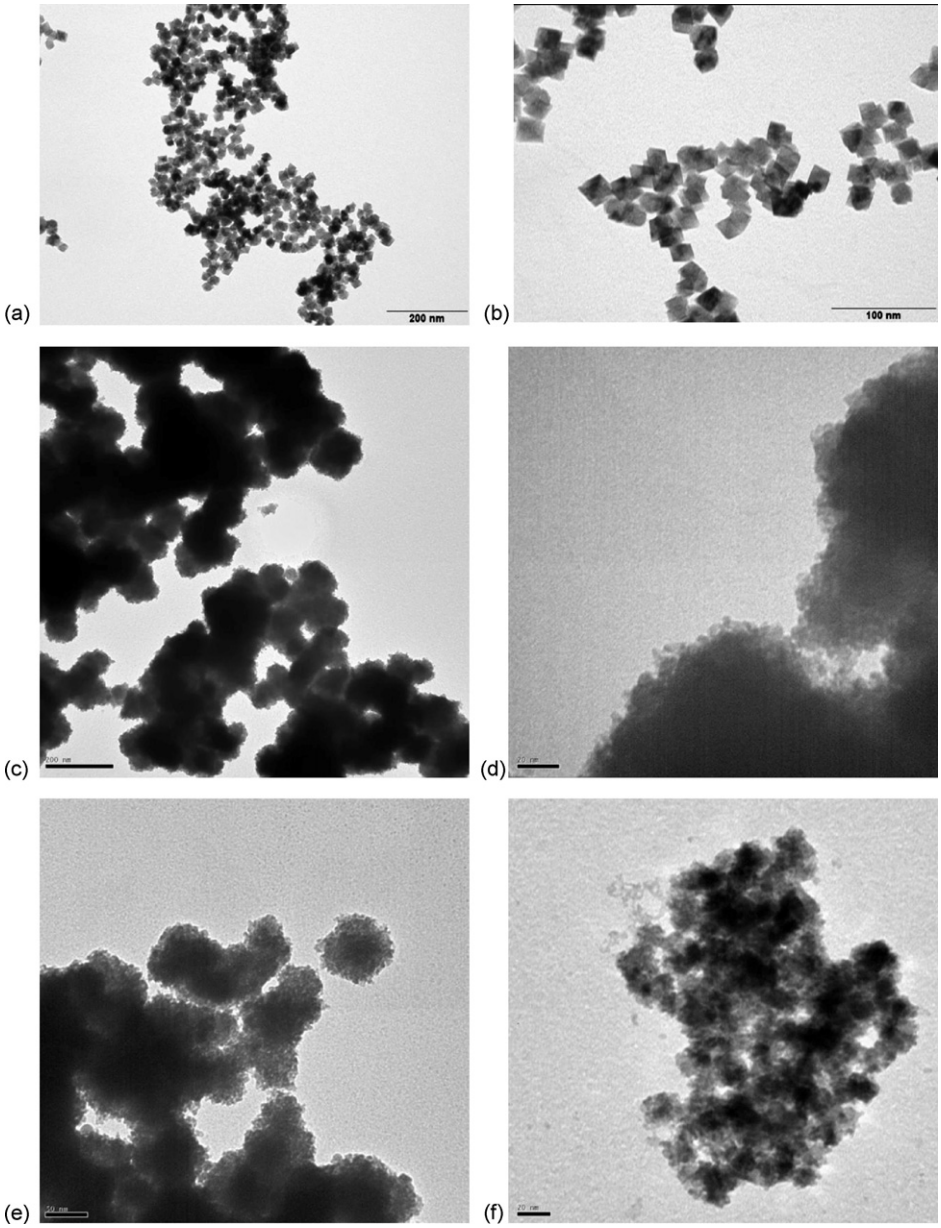

Fig. 5. TEM images of the initial CeO_2 nanoparticles (a) and (b); control CeO_2 nanoparticles in deionized water (c); CeO_2 nanoparticles after adsorption of chromium (VI) at different amplifications (d and e) and CeO_2 nanoparticles after desorption with 0.1 M NaOH eluent (e).

3.6. Bioluminescent test

The bioluminescent test is broadly used to evaluate the potential harmful effects of effluents discharged into surface waters [25]. Some proposed regulations set limit values for bioluminescent toxicity at 25 Equitox/m^3 [44]. The IC_{50} obtained for the Cr(VI) solution was 1.92 mg/l at 5 min exposure time (Table 4). In the case of CeO_2 nanoparticles the IC_{50} value obtained was 21.76 mg/l. The CeO_2 nanoparticles are positively charged at neutral pH and thus display a strong electrostatic attraction towards bacterial outer membranes. In this sense, Thill et al. [45] suggest that the first step for toxicity in *Escherichia coli* bacteria is the adsorption of it by the CeO_2 nanoparticles. The authors's study concluded that direct contact between the *E. coli* and the CeO_2 nanoparticles need to be assumed for CeO_2 cytotoxicity to occur and that the reduction of the nanoparticles occurs at or close to the surface of the bacteria and may be associated with cytotoxicity. The toxicity of the suspension obtained from an adsorption process after 3 h of reaction (37.5 mg/l of initial chromium) was 19.72 mg/l at 5 min exposure time. The differences between them (21.76 mg/l and 19.72 mg/l) and the high toxicity of the chromium solution (1.92 mg/l) suggest that the chromium adsorbed on the CeO_2 nanoparticles reduce the intrinsic chromium toxicity against the bacteria tested. Even though after 15 min of exposure time the IC_{50} diminish to 13.6 mg/l, and the IC_{50} for chromium solution also diminish at this time. A study of the toxicity of these nanoparticles at longer periods of

Table 4
Half maximal inhibitory concentration (IC_{50}) of a 30 mg/l chromium solution, initial CeO_2 nanoparticles and CeO_2–Cr(VI) suspension.

	IC_{50} (mg/l)	IC_{50} (mg/l)
Compounds	5 min	15 min
Cr(VI) solution	1.92	1.2
CeO_2 nanoparticles suspension	21.76	25.16
CeO_2–Cr(VI) suspension	19.72	13.6

time has to be done in order to know the possible environment impact. A dissolution process or aggregation phenomenon has to be in account.

4. Conclusions

The results obtained in this study demonstrate that the use of the cerium oxide nanoparticles synthesized can be an excellent option for the removal of low amounts of dissolved chromium VI in the purification of drinking water or in the re-use of wastewater. The agglomeration of nanoparticles during the adsorption process allows the use of common technologies in wastewater procedure to eliminate them. The adsorption of chromium onto nanoparticles is well described by the Freundlich isotherm, whereas kinetics corresponds to a pseudo-second-order equation. Both facts ensure a practically complete removal of chromium under the conditions tested. Following the treatment process, nanoparticles can be removed from water by centrifugation, whereas chromium can be desorpted using sodium hydroxide, closing the cycle of chromium removal, although some morphological changes are observed in the nanoparticles used. Of course, other parameters influencing the adsorption process such as pH, ionic strength, and temperature can the object of further studies. Finally, the toxicity of the resulting solutions is not significantly altered using this treatment.

Acknowledgements

Financial support was provided by the Spanish Ministerio de Medio Ambiente y Medio Rural y Marino (Project Exp. 007/RN08/03.1). Sonia Recillas and Joan Colón thank Universitat Autònoma de Barcelona for the award of a post-doctoral and predoctoral fellowship respectively.

References

[1] N. Ichinose, Y. Ozaki, S. Kashu, Superfine Particle Technology, Springer, London, 1992.
[2] P.V. Kamat, Photophysical, photochemical and photocatalytic aspects of metal nanopartícule, J. Phys. Chem. B 106 (2002) 7729–7744.
[3] P.K. Stoimenov, R.L. Klinger, G.L. Marchin, K.J. Klabunde, Metal oxide nanoparticles as bactericidal agents, Langmuir 18 (2002) 6679–6686.
[4] S.W. Cao, Y.J. Zhu, Hierarchically nanostructured α-Fe_2O_3 hollow spheres: preparation, growth mechanism, photocatalytic property, and application in water treatment, J. Phys. Chem. C 112 (2008) 6253–6257.
[5] H.M. Chen, J.H. He, Facile synthesis of monodisperse manganese oxide nanostructures and their application in water treatment, J. Phys. Chem. C 112 (2008) 17540–17545.
[6] D.K. Tiwari, J. Behari, P. Sen, Application of nanoparticles in waste water treatment, World Appl. Sci. J. 3 (2008) 417–433.
[7] D. Paustenbach, B. Finley, F. Mowat, B. Kerger, Human health risk and exposure assessment of chromium (VI) in tap water, J. Toxicol. Environ. Health A 66 (2003) 1295–1339.
[8] Council Directive 98/83/EC, On the quality of water intended for human consumption, Off. J. L 330 (November) (1998) 0032–0054, 05/12/1998.
[9] M.A. Olazabal, N.P. Nikolaidis, S.A. Suib, J.M. Madariaga, Precipitation equilibria of the chromium(VI)/iron(III) system and spectroscopic characterization of the precipitates, Environ. Sci. Technol. 31 (1997) 2898–2902.
[10] Z.H. Ai, Y. Chen, L.Z. Zhang, J.R. Qiu, Efficient removal of Cr(VI) from aqueous solution with Fe@Fe_2O_3 core–shell nanowires, Environ. Sci. Technol. 42 (2008) 6955–6960.
[11] M.J.S. Yabe, E. Oliveira, Heavy metals removal in industrial effluents by sequential adsorbent treatment, Adv. Environ. Res. 7 (2003) 263–272.
[12] P.A. Kumar, M. Ray, S. Chakraborty, Hexavalent chromium removal from wastewater using aniline formaldehyde condensate coated silica gel, J. Hazard. Mater. 143 (2007) 24–32.
[13] K. Selvi, S. Pattabhi, K. Kadirvelu, Removal of Cr(VI) from aqueous solution by adsorption onto activated carbon, Bioresour. Technol. 80 (2001) 87–89.
[14] Z. Hu, L. Lei, Y. Li, Y. Ni, Chromium adsorption of high performance activated carbon from aqueous solution, Sep. Purif. Technol. 31 (2003) 13–18.
[15] S.E. Bailey, T.J. Olin, R.M. Bricka, D.D. Adrian, A review of potentially low-cost sorbents for heavy metals, Water Res. 33 (1999) 2469–2479.
[16] S.-H. Huang, D.-H. Chen, Rapid removal of heavy metal cations and anions from aqueous solutions by an amino-functionalized magnetic nano-adsorbent, J. Hazard. Mater. 163 (2009) 174–179.
[17] L.-S. Zhong, J.-S. Hu, A.-M. Cao, Q. Liu, W.-G. Song, L.-J. Wan, 3D flowerlike ceria micro/nanocomposite structure and its application for water treatment and CO removal, Chem. Mater. 19 (2007) 1648–1655.
[18] Z.C. Di, J. Ding, X.J. Peng, Y.H. Li, Z.K. Luan, J. Liang, Chromium adsorption by aligned carbon nanotubes supported ceria nanopartícules, Chemosphere 62 (2006) 861–865.
[19] H.I. Xiao, Z.H. Ai, L.Z. Zhang, Nonaqueous sol–gel synthesized hierarchical CeO_2 nanocrystal microspheres as novel adsorbents for wastewater treatment, J. Phys. Chem. C 113 (38) (2009) 16625–16630.
[20] S.C. Laha, R. Ryoo, Synthesis of thermally stable mesoporous cerium oxide with nanocrystalline frameworks using mesoporous silica templates, Chem. Commun. 17 (2003) 2138–2139.
[21] S.C. Kuiry, S. Patil, S. Deshpande, S. Seal, Spontaneous self-assembly of cerium oxide nanoparticles to nanorods through supraaggregate formation, J. Phys. Chem. B 109 (2005) 6936–6939.
[22] M. Gutierrez, J. Etxebarria, L. Fuentes, Evaluation of wastewater toxicity: comparative study between Microtox® and activated sludge oxygen uptake inhibition, Water Res. 36 (2002) 919–924.
[23] F. Zhang, Q. Jin, S.W. Chan, Ceria nanoparticles: size, size distribution, and shape, J. Appl. Phys. 95 (2004) 4319–4326.
[24] A. Greenberg, J. Connors, D. Jenkins, Standard Methods for the Examination of Water and Wastewater, 15th ed., American Public Health Association, USA, 1981, pp. 187–190.
[25] DIN 38412, Determination of the inhibitory effect of wastewater on the light emission of *Photobacterium phosphoreum* (test using preserved luminescent bacteria), part 34, 1991.
[26] A.K. Pandey, V. Misra, A.K. Srimal, Removal of chromium and reduction of toxicity to microtox system from tannery effluent by the use of calcium alginate beads containing humic acid, Chemosphere 51 (2003) 329–333.
[27] A. Trovarelli, Catalysis by Ceria and Related Materials, Imperial College Press, London, 2002.
[28] C.R. Stanek, A.H.H. Tan, S.L. Owens, R.W. Grimes, Atomistic simulation of CeO_2 surface hydroxylation: implications for glass polishing, J. Mater. Sci. 43 (2008) 4157–4162.
[29] S. Bernal, J.J. Calvino, M.A. Cauqui, J.M. Gatica, C. Larese, J.A. Pérez Omil, J.M. Pintado, Some recent results on metal/support interaction effects in NM/CeO_2 (NM: noble metal) catalysts, Catal. Today 50 (1999) 175–206.
[30] S. Carrettin, P. Concepción, A. Corma, J.M. López Nieto, V.F. Puntes, Nanocrystalline CeO_2 increases the activity of Au for CO oxidation by two orders of magnitude, Angew. Chem. Int. Ed. 43 (2004) 2538–2540.
[31] F. Esch, S. Fabris, L. Zhou, T. Montini, C. Africh, P. Fornasiero, G. Comelli, R. Rosei, Electron localization determines defect formation on ceria substrates, Science 309 (2005) 752–755.
[32] J.Y. Chane-Ching, M. Airiau, A. Sahibed-dine, M. Daturi, E. Brendlé, F. Ozil, A. Thorel, A. Corma, Surface characterization and properties of ordered arrays of CeO_2 nanoparticles embedded in thin layers of SiO_2, Langmuir 21 (2005) 1568–1574.
[33] E.G. Heckert, S. Seal, W.T. Self, Fenton-like reaction catalyzed by the rare earth inner transition metal cerium, Environ. Sci. Technol. 42 (2008) 5014–5019.
[34] P. Yuan, M. Fan, D. Yang, H. He, D. Liu, A. Yuan, J. Zhu, T. Chen, Montmorillonite-supported magnetite nanoparticles for the removal of hexavalent chromium [Cr(VI)] from aqueous solutions, J. Hazard. Mater. 166 (2009) 821–829.
[35] J.G. Strom Jr., H. Won Jun, Kinetics of hydrolysis of methenamine, J. Pharm. Sci. 69 (1980) 1261–1263.
[36] A.J. Allen, V.A. Hackley, P.R. Jemian, J. Ilavsky, J.M. Raitano, S.-W. Chan, In situ ultra-small-angle X-ray scattering study of the solution-mediated formation and growth of nanocrystalline ceria, J. Appl. Cryst. 41 (2008) 918–929.
[37] I. Langmuir, The adsorption of gases on plane surfaces of glass, mica and platinum, J. Am. Chem. Soc. 40 (1918) 1361–1403.
[38] Y.S. Ho, G. McKay, The kinetics of sorption of divalent metal ions onto sphagnum moss peat, Water Res. 34 (2000) 735–742.
[39] S.V.N.T. Kuchibhatla, A.S. Karakoti, S. Seal, Hierarchical assembly of inorganic nanostructure building blocks to octahedral superstructures – a true template-free self-assembly, Nanotechnology 18 (2007) 075303.
[40] K. Kimura, S. Takashima, H. Ohshima, Molecular approach to the surface potential estimate of thiolate-modified gold nanopartícules, J. Phys. Chem. B 106 (2002) 7260–7266.
[41] T. Laaksonen, P. Ahonen, C. Johans, K. Kontturi, Stability and electrostatics of mercaptoundecanoic acid-capped gold nanoparticles with varying counterion size, ChemPhysChem 7 (2006) 2143–2149.
[42] B. Mukhopadhyaya, J. Sundq, R.J. Schmitzc, Removal of Cr(VI) from Cr-contaminated groundwater through electrochemical addition of Fe(II), J. Environ. Manage. 82 (2007) 66–76.
[43] C.T. Campbell, C.H.F. Peden, Oxygen vacancies and catalysis on ceria surfaces, Science 309 (2005) 752–755.
[44] R. Barrena, E. Casals, J. Colón, X. Font, A. Sánchez, V. Puntes, Evaluation of model nanoparticles eco-toxicity, Chemosphere 75 (2009) 850–857.
[45] A. Thill, O. Zeyons, O. Spalla, F. Chauvat, J. Rose, M. Auffan, A.M. Flank, Cytotoxicity of CeO_2 nanoparticles for *Escherichia coli*, Environ. Sci. Technol. 40 (2006) 6151–6156.